REGULAR ARTICLE

blood advances

EHBP1L1, an apicobasal polarity regulator, is critical for nuclear polarization during enucleation of erythroblasts

Ji Wu,[1,*] Kenta Moriwaki,[2,*] Tatsuya Asuka,[3] Ritsuko Nakai,[4] Satoshi Kanda,[1] Manabu Taniguchi,[1] Tatsuki Sugiyama,[5] Shin-ichiro Yoshimura,[1] Masataka Kunii,[1] Takashi Nagasawa,[5] Naoki Hosen,[4] Eiji Miyoshi,[3] and Akihiro Harada[1]

[1]Department of Cell Biology, Graduate School of Medicine, Osaka University, Suita, Japan; [2]Department of Biochemistry, Toho University School of Medicine, Tokyo, Japan; [3]Department of Molecular Biochemistry and Clinical Investigation, [4]Department of Hematology and Oncology, and [5]Laboratory of Stem Cell Biology and Developmental Immunology, Graduate School of Medicine, Osaka University, Suita, Japan

Key Points

- EHBP1L1 promotes nuclear polarization and subsequent enucleation of erythroblasts in coordination with Rab10, Bin1, and dynamin.
- EHBP1L1 maintains the proper morphology and structural stability of erythrocytes.

Cell polarity, the asymmetric distribution of proteins and organelles, is permanently or transiently established in various cell types and plays an important role in many physiological events. epidermal growth factor receptor substrate 15 homology domain-binding protein 1–like 1 (EHBP1L1) is an adapter protein that is localized on recycling endosomes and regulates apical-directed transport in polarized epithelial cells. However, the role of EHBP1L1 in nonepithelial cells, remains unknown. Here, *Ehbp1l1*$^{-/-}$ mice showed impaired erythroblast enucleation. Further analyses showed that nuclear polarization before enucleation was impaired in *Ehbp1l1*$^{-/-}$ erythroblasts. It was also revealed that EHBP1L1 interactors Rab10, Bin1, and dynamin were involved in erythroblast enucleation. In addition, *Ehbp1l1*$^{-/-}$ erythrocytes exhibited stomatocytic morphology and dehydration. These defects in erythroid cells culminated in early postnatal anemic lethality in *Ehbp1l1*$^{-/-}$ mice. Moreover, we found the mislocalization of nuclei and mitochondria in the skeletal muscle cells of *Ehbp1l1*$^{-/-}$ mice, as observed in patients with centronuclear myopathy with genetic mutations in Bin1 or dynamin 2. Taken together, our findings indicate that the Rab8/10-EHBP1L1-Bin1-dynamin axis plays an important role in multiple cell polarity systems in epithelial and nonepithelial cells.

Introduction

Cell polarity is a fundamental feature of cells characterized by the asymmetric morphology and distribution of organelles and molecules, such as proteins and lipids. The establishment of cell polarity is indispensable for diverse cellular events in various cell types.[1] There are multiple cell polarity systems that are categorized into 2 types: permanent cell polarity (eg, apicobasal polarity in epithelial cells) and transient cell polarity (eg, front-rear polarity in migrating cells). Defects in these polarity systems result in embryonic lethality and tumor progression.[2]

The nuclei are asymmetrically positioned in various cell types.[3] For instance, in muscle fibers, the nuclei are positioned at the periphery. In addition, the position of the nuclei changes dynamically when transient cell polarity is established. This dynamic establishment of cell and nuclear polarity is also observed during mammalian erythropoiesis, a process by which erythrocytes are generated from erythroid progenitors.

Submitted 12 September 2022; accepted 31 March 2023; prepublished online on *Blood Advances* First Edition 12 April 2023. https://doi.org/10.1182/bloodadvances.2022008930.

*J.W. and K.M. contributed equally to this study.

Data are available on request from the corresponding authors, Kenta Moriwaki (kenta.moriwaki@med.toho-u.ac.jp) and Akihiro Harada (aharada@acb.med.osaka-u.ac.jp).

The full-text version of this article contains a data supplement.

Early erythroid progenitors, burst-forming units-erythroid, differentiate into erythroblasts in several differentiation stages.[4] In erythroblasts, nuclei become condensed and asymmetrically positioned during differentiation and are eventually extruded, which produces reticulocytes and pyrenocytes.[5] Finally, reticulocytes mature into erythrocytes through membrane remodeling and the removal of organelles and macromolecules, such as proteins and nucleic acids. Erythroblast enucleation is a complex process coordinated by multiple regulators, such as epigenomic regulators,[6,7] Rho GTPases,[8,9] cytoskeletal proteins,[9-12] and cell polarity regulators.[13,14] Previous studies have shown that membrane trafficking is a crucial mechanism that regulates the dynamic process of enucleation.[15-17] However, the detailed molecular mechanisms underlying the role of membrane trafficking in erythroblast enucleation remain unknown.

Rab proteins are Ras-like small GTPases that play essential roles in membrane trafficking. We previously found that Rab8-deficient mice exhibit defects in apical transport in intestinal epithelial cells.[18,19] Our subsequent study identified epidermal growth factor receptor substrate 15 homology domain-binding protein 1-like 1 (EHBP1L1) as a Rab8 effector protein that regulates epithelial apical transport.[20] EHBP1L1 interacts with Rab8 on recycling endosomes and recruits Bin1 and dynamin, which generate membrane curvature and sever the curved membrane to create vesicles, respectively. However, the role of EHBP1L1 in nonepithelial cells remains unknown.

Here, we found that the loss of EHBP1L1 caused defects in nuclear polarization and subsequent enucleation during terminal erythropoiesis. Downregulation of Rab10, which is another EHBP1L1-binding Rab protein, Bin1, and dynamin also impaired erythroblast enucleation. In addition, enucleated erythrocytes in EHBP1L1-deficient (*Ehbp1l1*$^{-/-}$) mice exhibited stomatocytic morphology. These deficiencies culminated in lethal anemia with excessive hemolysis in *Ehbp1l1*$^{-/-}$ mice. Furthermore, we found mislocalized nuclei and mitochondria in the muscle fibers of *Ehbp1l1*$^{-/-}$ mice, as observed in patients with centronuclear myopathy with genetic mutations in Bin1 or dynamin 2. Taken together, our findings suggest that the Rab8/10-EHBP1L1-Bin1-dynamin axis plays an important role in multiple cell polarity systems in epithelial and nonepithelial cells.

Methods

Mice

Ehbp1l1$^{-/-}$ mice were developed in our laboratory.[20] ICR mice were purchased from Japan SLC and CLEA Japan. All the mice were maintained under specific pathogen-free conditions in an animal facility at Osaka University. The experimental protocols were approved by the Institutional Committee for Experiments using animals (01-004-010) and recombinant DNA (04421). The genotypes of the mice were identified by polymerase chain reaction (F: GACAAAGAAAAGAGCTCCAGAGACC; R: CCTTGACAGTCCAATACAAGACCTG), followed by digestion with PstI.

Flow cytometry

Fetal livers were dispersed in Iscove modified Dulbecco medium (Wako, 098-16465) by gentle pipetting. The cell suspension was passed through a 77 μm filter paper and further through a 25 μm filter paper. The cells were stained with fluorescently labeled antibodies and 5 μg/mL Hoechst 33342 (Sigma-Aldrich, B2261). For staining with Annexin V, the cells were washed with Annexin V binding buffer (10 mM *N*-2-hydroxyethylpiperazine-*N*′-2-ethanesulfonic acid, 140 mM NaCl, and 2.5 mM $CaCl_2$) and then stained with FITC-conjugated Annexin V (BioLegend, 640906). The fluorescently labeled antibodies are listed in supplemental Table 1. For intracellular staining of EHBP1L1, after cell-surface staining, the cells were fixed with 3% paraformaldehyde for 20 minutes. The fixed cells were incubated in a permeabilization buffer (0.1% saponin and 5% normal donkey serum in phosphate-buffered saline) for 20 minutes. The cells were then stained with an anti-EHBP1L1 antibody[20] in a permeabilization buffer for 45 minutes. An equal amount of rabbit IgG (Wako, 148-09551) was used as a negative control. After washing, the cells were stained with Alexa Fluor 488–conjugated donkey anti-rabbit IgG (Invitrogen, A21206) in a permeabilization buffer for 45 minutes. The cells were analyzed using either a FACSCanto II (BD Biosciences) or ImageStreamX MK II (Amnis) flow cytometer. Data analysis was performed using the FlowJo (FlowJo) or IDEAS (Amnis) software.

MEDEP-BRC5 cell analysis

MEDEP-BRC5 cells were obtained from RIKEN BRC (RCB2911).[21] MEDEP-BRC5 cells were cultured in Iscove modified Dulbecco medium, supplemented with 15% fetal calf serum, 1× ITS liquid medium (Sigma-Aldrich, I3146), 50 μg/mL ascorbic acid (Sigma-Aldrich, A4403), 0.45 mM α-monothioglycerol (Wako, 195-15791), 50 ng/mL recombinant mouse stem cell factor (BioLegend, 579706), 1 μM dexamethasone (Sigma-Aldrich, D4902), 2 mM GlutaMAX (Gibco, 25050-061), 100 units per mL penicillin, and 100 μg/mL streptomycin (Wako, 168-23191). For differentiation, 5 units per mL erythropoietin (Kyowa Hakko Kirin) was added to the culture medium, stem cell factor and dexamethasone were removed, and the cells were cultured for 48 hours. Where indicated, dynasore (30 μM; Calbiochem, 324410) and Dyngo-4a (30 μM; Selleck, S7163) were added 24 hours before analysis. The differentiated cells were stained with FITC-conjugated anti-CD71 and allophycocyanin-conjugated anti-Ter119 antibodies, 5 μg/mL Hoechst 33342, and 50 μg/mL propidium iodide (Dojindo, 341-07881), and analyzed using a FACSCanto II flow cytometer. The fluorescently labeled antibodies are listed in supplemental Table 1.

Statistics

Statistical analysis was performed using an unpaired *t* test with Welch's correction, one-way or two-way analysis of variance. A *P* value of $<.05$ was considered to indicate a statistically significant difference. All statistical analyses were performed using Prism 9 (GraphPad software).

Results

Loss of EHBP1L1 causes lethal anemia

We previously developed *Ehbp1l1*$^{-/-}$ mice using the CRISPR/Cas9 system and reported that the mice died within a day of birth.[20] Here, we performed extended phenotypic analyses and found that although *Ehbp1l1*$^{-/-}$ mice were born at the expected Mendelian ratio (Figure 1A), all the mice were severely pale and did not survive for more than 1 day after birth (Figure 1B-C). In addition, we found that the number of erythrocytes in the peripheral

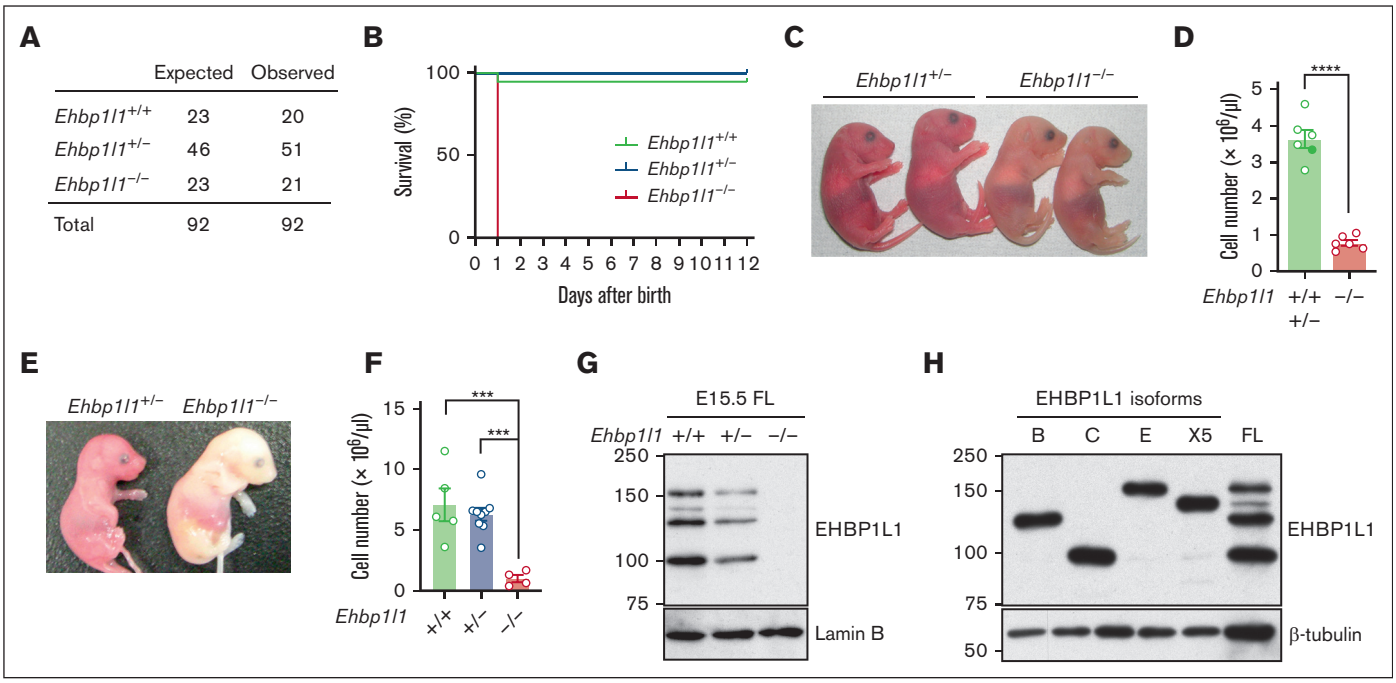

Figure 1. *Ehbp1l1*$^{-/-}$ mice exhibit lethal anemia. (A) The numbers of progenies with the indicated genotypes from *Ehbp1l1*$^{+/-}$ intercrosses are shown. (B) Survival curves of the progenies from *Ehbp1l1*$^{+/-}$ intercrosses are shown (*Ehbp1l1*$^{+/+}$: n = 18, *Ehbp1l1*$^{+/-}$: n = 47, *Ehbp1l1*$^{-/-}$: n = 19). (C,E) Representative pictures of *Ehbp1l1*$^{+/-}$ and *Ehbp1l1*$^{-/-}$ mice at P0 (the day of birth) (C) and E18.5 (E) are shown. (D,F) Total cell numbers in peripheral blood at P0 (D, *Ehbp1l1*$^{+/+}$ shown as a solid green circle: n = 1, *Ehbp1l1*$^{+/-}$ shown as open green circles: n = 5, *Ehbp1l1*$^{-/-}$: n = 6) and E18.5 (F, *Ehbp1l1*$^{+/+}$: n = 5, *Ehbp1l1*$^{+/-}$: n = 9, *Ehbp1l1*$^{-/-}$: n = 4) are shown. The data are presented as the means ± standard error of the mean (SEMs). (G) Whole-cell extracts (WCEs) from fetal livers (FL) of E15.5 embryos with the indicated genotypes were analyzed by western blotting using the indicated antibodies. (H) WCEs from *Ehbp1l1*$^{-/-}$ mouse embryonic fibroblasts transfected with pcDNA3 encoding EHBP1L1 isoform B, C, E, or X5 and WCEs from E14.5 mouse FL were subjected to western blotting. ***$P < .001$, ****$P < .0001$ (unpaired *t* test with Welch's correction in panel D; 1-way analysis of variance [ANOVA] in panel F).

blood was significantly reduced in neonatal *Ehbp1l1*$^{-/-}$ mice compared with *Ehbp1l1*$^{+/+}$ and *Ehbp1l1*$^{+/-}$ mice (Figure 1D). These results indicate that *Ehbp1l1*$^{-/-}$ mice exhibited severe anemia. Anemia was also observed in *Ehbp1l1*$^{-/-}$ embryos at embryonic day 18.5 (E18.5) (Figure 1E-F). Because *Ehbp1l1*$^{+/-}$ mice did not exhibit these abnormalities, they were included as control mice in this study.

Thirteen *Ehbp1l1* mRNA isoforms that encode 12 protein isoforms are listed in the NCBI database (supplemental Figure 1). Studies with our anti-EHBP1L1 antibody, which was generated using the purified EHBP1L1 proline-rich domain as an immunogen,[20] showed that 4 isoforms were expressed in the fetal liver at E15.5 (Figure 1G). All isoforms were absent in the *Ehbp1l1*$^{-/-}$ fetal liver (Figure 1G). By subcloning and DNA sequencing analysis, the expressed isoforms were identified as B, C, E, and X5 (Figure 1H).

EHBP1L1 regulates enucleation during terminal erythropoiesis

The developmental switching of β-globin gene expression is a critical event during normal erythropoiesis.[22] Gene expression of embryonic (*Hbb-bh1* and *Hbb-y*) and adult globins (*Hbb-b1*) was normal in *Ehbp1l1*$^{-/-}$ mice (supplemental Figure 2A). When we examined the peripheral blood using May-Grunwald Giemsa staining, we observed many circulating nucleated cells in *Ehbp1l1*$^{-/-}$ mice (Figure 2A). Flow cytometric analysis revealed that these nucleated cells were erythrocytes, as they expressed the erythrocyte marker, Ter119 (Figure 2B-C). During normal definitive erythropoiesis in the perinatal period, the nuclei of orthochromatic erythroblasts in the liver are extruded. To determine the role of EHBP1L1 in the production of enucleated erythrocytes, we examined the erythroid cell population at different stages of differentiation in the fetal liver (supplemental Figure 2B). Burst-forming units-erythroid differentiate into colony-forming units-erythroid, which further differentiate into proerythroblasts. During the differentiation of colony-forming units-erythroid into proerythroblasts, the expression levels of Ter119 and CD117 gradually increase and decrease, respectively (supplemental Figure 2B). Loss of EHBP1L1 did not affect the proportion and number of these erythroblast progenitors on any of the tested embryonic days (Figure 2D; supplemental Figure 2C). Proerythroblasts differentiate into basophilic, polychromatic, and eventually orthochromatic erythroblasts upon successive cell divisions.[23] Because both cell size and CD44 expression are reduced along this erythroblast maturation continuum,[24] we defined each erythroblast based on these 2 parameters, such that the erythroblast ratio (basophilic:polychromatic:orthochromatic) was 1:2:4 (supplemental Figure 2B). We found that the proportion and number of orthochromatic erythroblasts, but not basophilic and polychromatic erythroblasts, were significantly higher in *Ehbp1l1*$^{-/-}$ mice than control mice (Figure 2D-E; supplemental Figure 2C). In contrast, those of enucleated cells were significantly decreased in

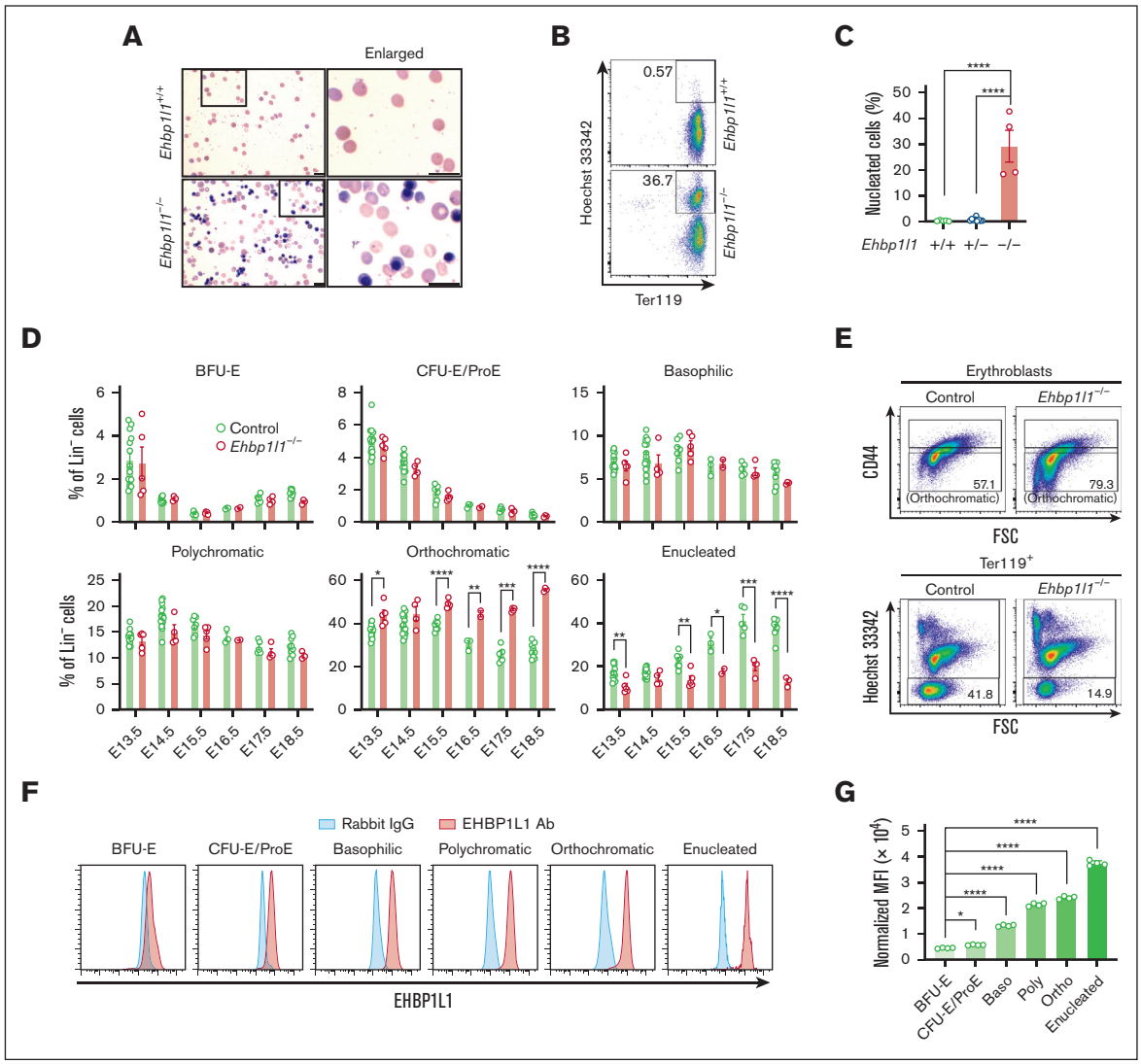

Figure 2. EHBP1L1 promotes erythroblast enucleation. (A) The peripheral blood collected from control and *Ehbp1l1*$^{-/-}$ P0 mice was subjected to May-Grunwald-Giemsa staining. Representative pictures are shown. The areas enclosed in the black squares were enlarged and are shown in the right panels. Scale bars: 10 μm. (B-C) The peripheral blood collected from mice with the indicated genotypes was analyzed by flow cytometry (*Ehbp1l1*$^{+/+}$: n = 5, *Ehbp1l1*$^{+/-}$: n = 9, *Ehbp1l1*$^{-/-}$: n = 4). Representative flow cytometry plots are shown. (D-E) Fetal liver cells (FLCs) from control and *Ehbp1l1*$^{-/-}$ embryos were analyzed by flow cytometry. N = 14 (E13.5), 16 (E14.5), 7 (E15.5), 3 (E16.5), 5 (E17.5), and 9 (E18.5) for control embryos. N = 5 (E13.5), 4 (E14.5), 5 (E15.5), 2 (E16.5), 4 (E17.5), and 3 (E18.5) for *Ehbp1l1*$^{-/-}$ embryos. The upper and lower flow cytometry plots in E show representative data for Lin^{-}Ter119^{high}Hoechst 33342^{+}AnnexinV^{-} erythroblasts and Lin^{-}Ter119^{high} cells, respectively. (F-G) FLCs from E13.5 ICR embryos were analyzed by flow cytometry (n = 4). Representative flow cytometry plots of erythroid cells at distinct stages of erythropoiesis are shown. The mean fluorescence intensity (MFI) of EHBP1L1 staining was normalized based on that of control rabbit IgG staining. The result is representative of 2 independent experiments. The data are presented as means ± SEMs for panels C-D,G. *$P < .05$; **$P < .01$; ***$P < .001$, ****$P < .0001$ (1-way ANOVA in panels C,G; unpaired *t* test with Welch's correction in panel D). BFU-E, burst-forming units-erythroid; CFU-E, colony-forming units-erythroid; ProE, proerythroblasts.

Ehbp1l1$^{-/-}$ mice. We also found that EHBP1L1 expression gradually increased during definitive erythropoiesis (Figure 2F-G; supplemental Figure 2D), implying the crucial role of EHBP1L1 during terminal erythroid differentiation. These results indicate that EHBP1L1 promotes the enucleation of erythroblasts without affecting early erythroid differentiation.

EHBP1L1 regulates erythroblast enucleation by promoting nuclear polarization

Erythroblast enucleation occurs on erythroblastic islands, consisting of a central macrophage surrounded by erythroblasts. Extruded nuclei, referred to as pyrenocytes, are engulfed by macrophages in a manner dependent on the expression of phosphatidylserine.[25] As EHBP1L1 was systemically deleted in *Ehbp1l1*$^{-/-}$ mice, we examined whether EHBP1L1 has a cell-intrinsic role in regulating erythroblast enucleation. We isolated Lin^{-}Ter119^{-}CD117^{+} erythroid progenitors and differentiated them into erythrocytes in vitro. We found that the enucleation of *Ehbp1l1*$^{-/-}$ erythroblasts was significantly reduced in this in vitro culture system (Figure 3A-B), indicating the erythroblast-intrinsic role of EHBP1L1 in enucleation.

During the final stage of erythroblast enucleation, F-actin is reported to accumulate at the constriction site between the

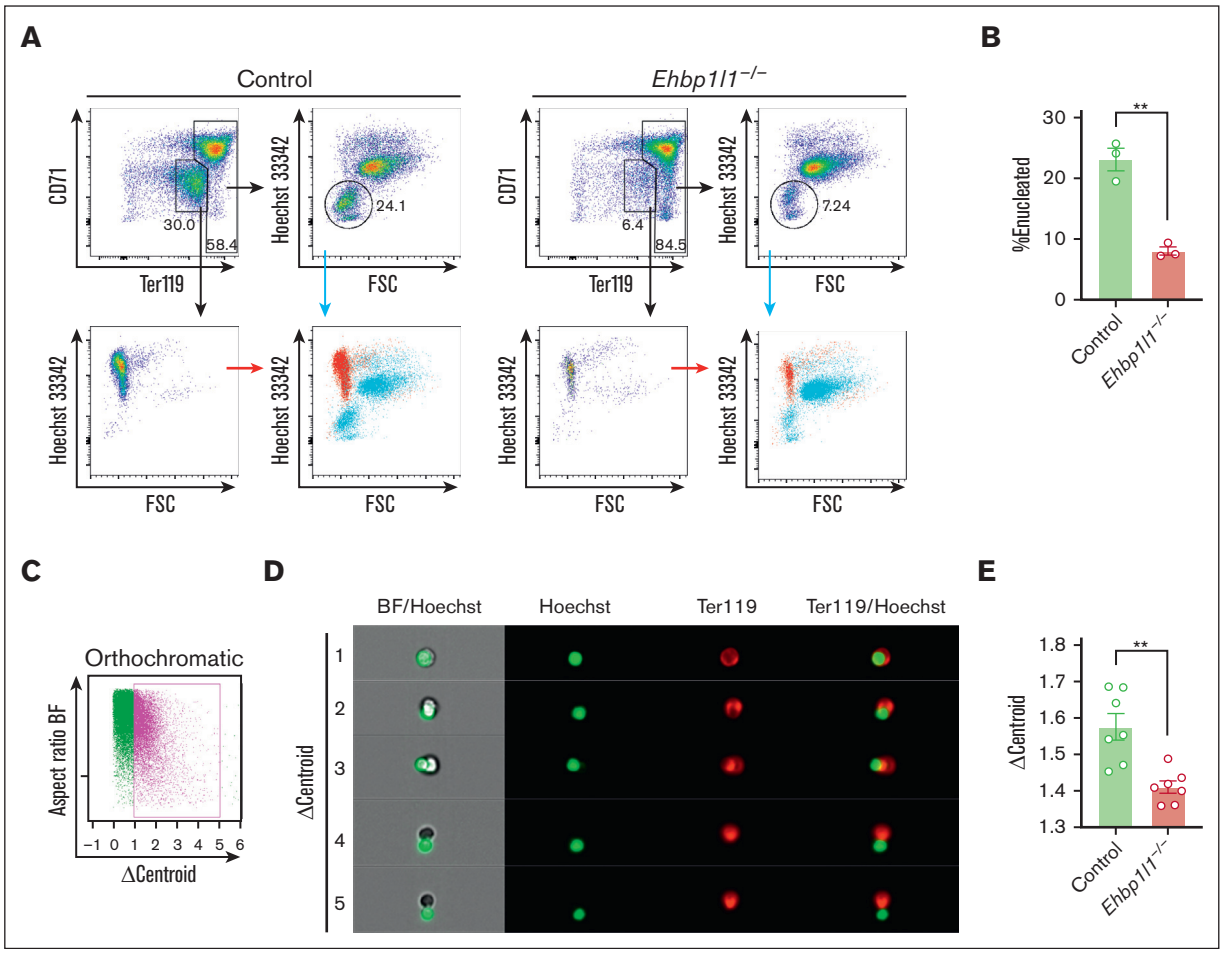

Figure 3. EHBP1L1 promotes nuclear polarization during terminal erythroid maturation. (A-B) Lin$^-$Ter119$^-$CD117$^+$ erythroid progenitors from control and *Ehbp1l1*$^{-/-}$ embryos (n = 3) were differentiated as described in the "Materials and methods" section. Representative flow cytometry plots of PI$^-$ cells are shown. The percentages of Hoechst 33342$^-$ cells among Ter119^{high} cells are shown in a bar-dot plot (B). The data are representative of 2 independent experiments. (C-E) FLCs from control and *Ehbp1l1*$^{-/-}$ embryos (E17.5, n = 7 pooled from 3 independent experiments) were analyzed using imaging flow cytometry. A representative flow cytometry plot of Ter119^{high}Hoechst 33342$^+$CD44^{low} orthochromatic erythroblasts is shown (C). Representative images of enucleating cells are shown (D). The average Δcentroid of the cells gated in the pink square in the flow cytometry plot is shown in a bar-dot plot (E). The data are presented as the means ± SEMs for panels B,E. $^{**}P < .01$ (unpaired *t* test with Welch's correction). BF, bright field.

extruding nucleus and reticulocyte, which is believed to drive constriction of the plasma membrane.[26] We observed that the localization of F-actin was similar between control and *Ehbp1l1*$^{-/-}$ erythroblasts (supplemental Figure 3A). Nuclear polarization before the constriction of the plasma membrane is indispensable for enucleation. To reveal the role of EHBP1L1 in this process, we performed imaging flow cytometry. Nuclear polarization can be assessed by measuring Δcentroid, which indicates the distance between the geometrical centers of the nucleus and cell. We found that the Δcentroid in orthochromatic erythroblasts was significantly lower in *Ehbp1l1*$^{-/-}$ mice than in control mice (Figure 3C-E), indicating impaired nuclear polarization in *Ehbp1l1*$^{-/-}$ erythroblasts. A similar reduction in Δcentroid was observed when cells were treated with an inhibitor of phosphatidylinositol-3-kinase, as described in a previous study (supplemental Figure 3B).[14] These results suggest that EHBP1L1 promotes nuclear polarity during enucleation but does not generate forces to constrict the plasma membrane.

The Rab10-EHBP1L1-Bin1-dynamin 2 axis regulates erythroblast enucleation

We previously revealed that EHBP1L1 localizes to recycling endosomes, where it bridges Rab8 and the Bin1-dynamin complex to regulate apical transport.[20] Here, we observed that EHBP1L1 was colocalized with CD71/transferrin receptor 1 (TfR1), which is a marker for recycling endosomes, during erythroblast enucleation, but was not colocalized with the lysosome marker LAMP2 (Figure 4A; supplemental Figure 4A). Cell-surface expression of CD71 on enucleating erythroblasts was normal in the absence of EHBP1L1 (supplemental Figure 4B). EHBP1L1 was also partially colocalized with Rab8 (supplemental Figure 4C). Although these results suggested that EHBP1L1 cooperates with Rab8 on recycling endosomes to promote enucleation, the Rab8a/b double-deficient mice that we previously developed did not exhibit an anemic phenotype.[18] We and others have shown that EHBP1L1 interacts with other Sec4/Rab8 subfamily members, such as

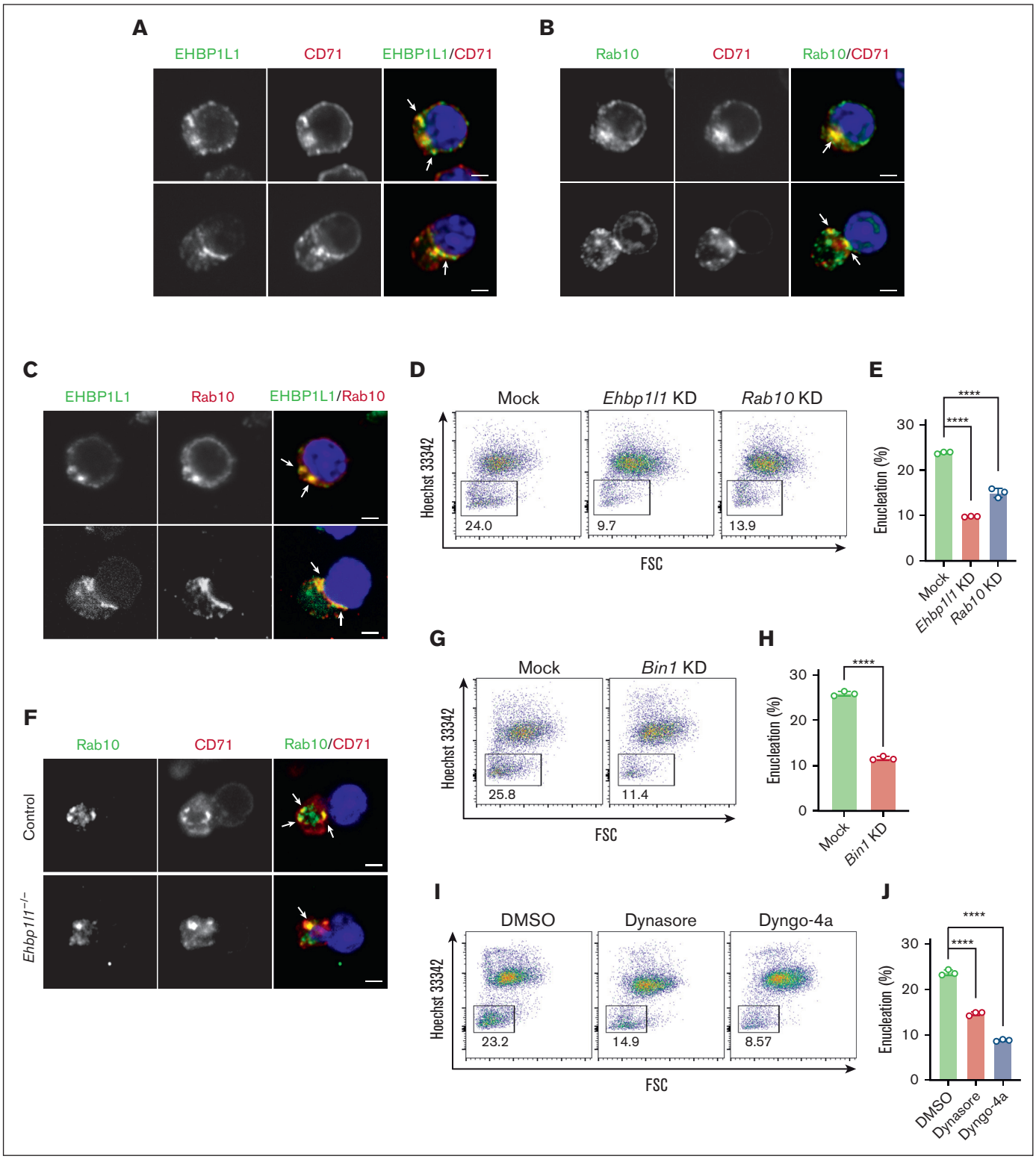

Figure 4. EHBP1L1 cooperates with Rab10, Bin1, and dynamin to promote erythroblast enucleation. (A-C,F) Lin$^-$Ter119$^-$CD117$^+$ erythroid progenitors from ICR embryos (A-C) and embryos with the indicated genotypes (F) were differentiated as described in the "Materials and methods" section. The differentiated erythroblasts were subjected to immunofluorescence staining for the indicated proteins. The white arrows indicate representative colocalization events. Nuclei (blue) were stained with 4′,6-diamidino-2-phenylindole (DAPI). Bars: 2 μm. (D-E,G-J) MEDEP-BRC5 cells with shRNA-mediated knockdown (KD) of *Ehbp1l1*, *Rab10*, or *Bin1* (D-E,G-H) or with dynamin inhibitor treatment (I-J) were differentiated and analyzed by flow cytometry. The cells were treated with the dynamin inhibitors (30 μM) for the last 24 hours of differentiation (I-J). Representative flow cytometry plots of PI$^-$Ter119^{high} cells are shown. The percentage of Hoechst 33342$^-$ cells among PI$^-$Ter119^{high} cells is shown in a bar-dot plot (triplicates; E,H,J). The data are representative of more than 3 independent experiments. The data are presented as means ± standard deviation (SDs). ****$P < .0001$ (1-way ANOVA in panel E,J; unpaired *t* test with Welch's correction in panel H).

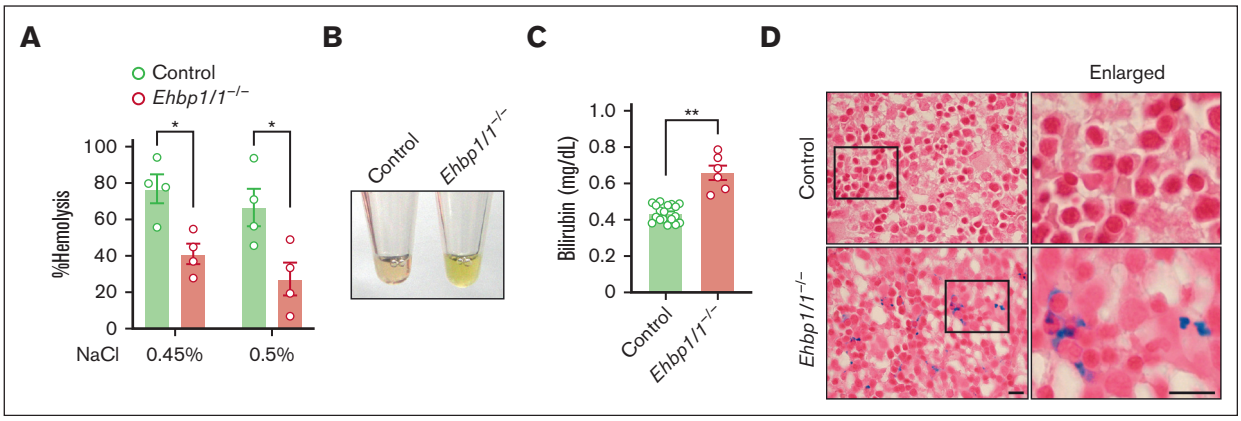

Figure 5. EHBP1L1-deficient erythrocytes are prone to hemolysis. (A) The percentage of hemolysis in enucleated erythrocytes isolated from the peripheral blood of control and *Ehbp1l1*$^{-/-}$ E18.5 embryos when exposed to the indicated hypotonic solutions is shown (n = 4). The data are representative of 3 independent experiments. (B) A representative picture of serum from control and *Ehbp1l1*$^{-/-}$ E18.5 embryos is shown. (C) The bilirubin concentration in serum from control (n = 19) and *Ehbp1l1*$^{-/-}$ (n = 6) E18.5 embryos and P0 mice was determined by using the UnaG protein. (D) Representative images of Berlin blue staining of liver tissues are shown. The areas enclosed in the black squares were enlarged. Scale bars: 10 μm. The data are presented as means ± SEMs for panels A,C. *$P < .05$, **$P < .01$ (unpaired *t* test with Welch's correction).

Rab10, Rab13, and Rab15.[20,27,28] Publicly available RNA sequencing data of mouse erythroblasts at distinct stages of terminal erythroid differentiation indicated the expression of Rab8b, Rab10, and, to a lesser extent, Rab8a, but not Rab13 and Rab15 (supplemental Figure 4D) (GSE53983).[29,30] The lack of or negligible levels of Rab13 and Rab15 expression were confirmed by RT-PCR analysis of in vitro–differentiated erythroblasts and mouse fetal livers (supplemental Figure 4E). Therefore, we hypothesized that EHBP1L1 would cooperate with Rab10 to regulate erythroblast enucleation. To test this hypothesis, we examined the localization of Rab10 in erythroblasts and found that it was colocalized with CD71/TfR1 but not with LAMP2 (Figure 4B; supplemental Figure 4F). We also observed the colocalization of Rab10 and EHBP1L1 (Figure 4C). Although some proteins are evenly distributed between reticulocytes and pyrenocytes after enucleation, others exhibit uneven distribution between the 2 cell types.[31] Most of EHBP1L1 and Rab10 were retained in reticulocytes (Figure 4A-C). The distribution of Band3 and β1-integrin, which mainly segregate into reticulocytes and pyrenocytes, respectively, was not affected by the loss of EHBP1L1 (supplemental Figure 4G-H), indicating that the loss of EHBP1L1 does not cause a global defect in protein transport.

To delineate the role of Rab10 in erythroblast enucleation, we used the mouse embryonic stem cell–derived erythroid progenitor cell line MEDEP-BRC5, which undergoes efficient enucleation upon the addition of erythropoietin (supplemental Figure 5A).[21] We confirmed the promoting effect of EHBP1L1 on enucleation in MEDEP-BRC5 cells via shRNA-mediated knockdown (Figure 4D-E; supplemental Figure 5B). Importantly, we found that the shRNA-mediated knockdown of Rab10 resulted in a significant reduction in enucleation efficiency (Figure 4D-E; supplemental Figure 5B). Because the deletion of EHBP1L1 did not affect the localization of Rab10 on CD71/TfR1-positive recycling endosomes (Figure 4F), Rab10 probably lies upstream of EHBP1L1. Furthermore, we found that enucleation was significantly inhibited by the knockdown of Bin1, which is the downstream effector of EHBP1L1 (Figure 4G-H; supplemental Figure 5C). Amphiphysin, a close family member of Bin1, was expressed at very low levels in erythroblasts and mouse fetal livers (supplemental Figure 4E). A previous study reported that the inhibition of dynamin, which is another downstream effector of EHBP1L1, by the chemical inhibitor dynasore reduced erythroblast enucleation efficiency.[16] Because off-target effects of dynasore have been reported,[32] we used a different dynamin inhibitor, Dyngo-4a, which has higher potency and a distinct inhibitory mechanism.[33] Similar to dynasore, Dyngo-4a significantly inhibited enucleation (Figure 4I-J). Notably, the downregulation of Rab10, Bin1, and dynamin in MEDEP-BRC5 cells did not affect their differentiation into Ter119^{high} cells (supplemental Figure 5D-F), suggesting that these proteins play dispensable roles in early erythroid differentiation. Furthermore, enucleation efficiency in the human embryonic stem cell–derived erythroid progenitor cell line HUDEP-2 was significantly reduced by the shRNA-mediated knockdown of *EHBP1L1* (supplemental Figure 5G-I), indicating the important role of EHBP1L1 in human erythropoiesis. Because dynamin 2 was highly expressed in erythroblasts (supplemental Figure 4E), these results suggest that the Rab10-EHBP1L1-Bin1-dynamin 2 axis plays a critical role in erythroblast enucleation.

Loss of EHBP1L1 results in excessive hemolysis

When we examined the morphology of erythrocytes in the peripheral blood, we noted the presence of many stomatocytes, which were characterized by a central biconcave slit in *Ehbp1l1*$^{-/-}$ mice (Figure 2A). Stomatocytes are abnormal erythrocytes with an abnormal intracellular water content.[34] Although stomatocytes are formed because of either overhydration or dehydration, *Ehbp1l1*$^{-/-}$ enucleated erythrocytes were likely dehydrated, as they were more resistant to osmotic stress (Figure 5A; supplemental Figure 6A). On performing new methylene blue staining of the peripheral blood to distinguish between reticulocytes and erythrocytes, we found that erythrocytes, but not reticulocytes, exhibited stomatocytic morphology (supplemental Figure 6B). In addition, in vitro–differentiated enucleated cells, which are mostly reticulocytes, did not show stomatocytic morphology (supplemental Figure 6C). These results suggest that EHBP1L1 plays a role in maintaining the morphology of mature erythrocytes.

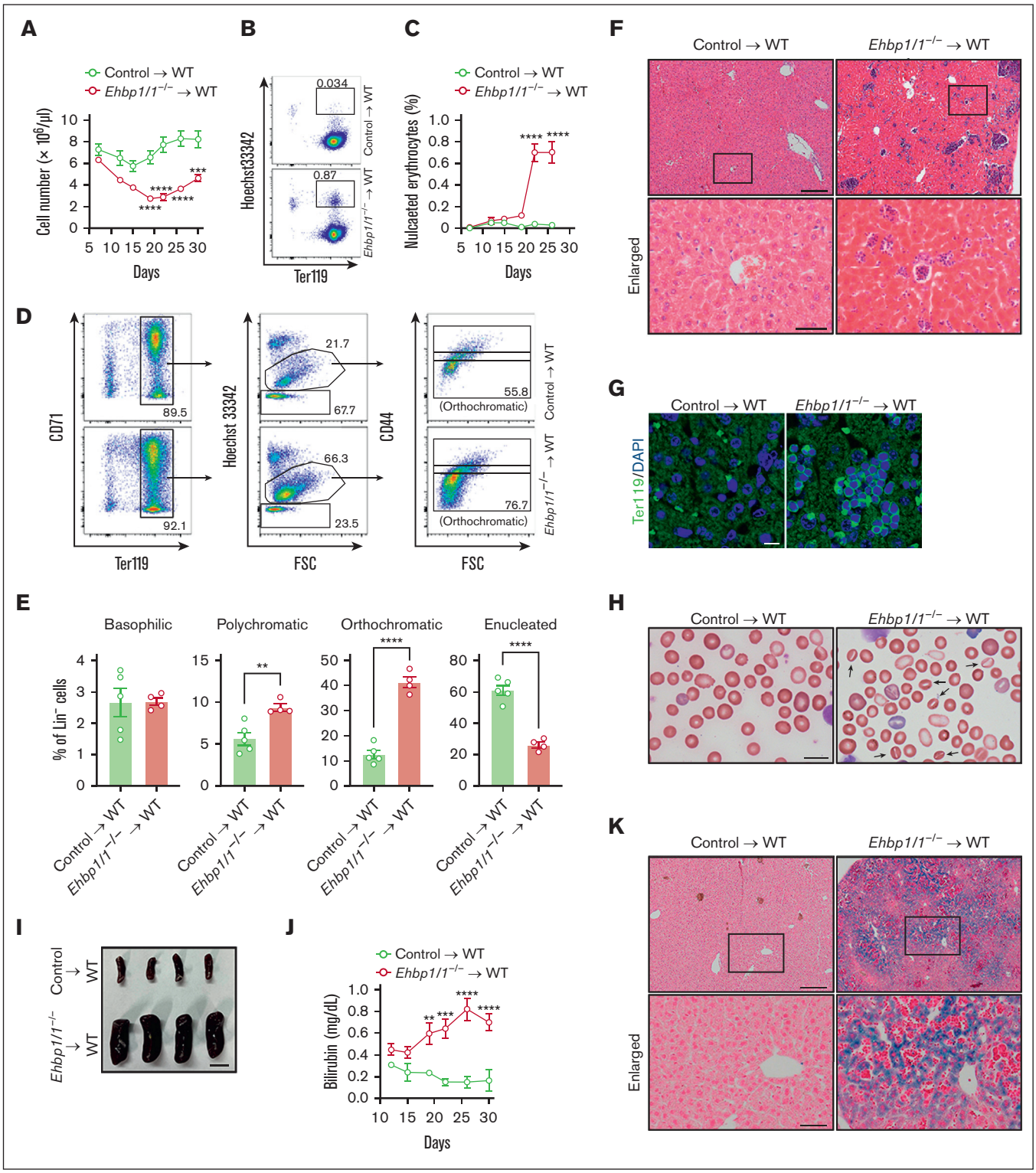

Figure 6. Mice transplanted with *Ehbp1l1*$^{-/-}$ hematopoietic cells exhibited impaired erythroblast enucleation and hemolytic anemia. FLCs from *Ehbp1l1*$^{+/+}$ and *Ehbp1l1*$^{-/-}$ E14.5 embryos were transplanted into irradiated wild-type mice. (A) Total cell numbers in the peripheral blood at indicated days after transplantation (control: n = 5, *Ehbp1l1*$^{-/-}$: n = 4). (B-E) Peripheral blood (B-C) and bone marrow cells (D-E) collected at indicated (B-C) and 35 days (D-E) after transplantation, respectively, were analyzed by flow cytometry (control: n = 5, *Ehbp1l1*$^{-/-}$: n = 4). Representative flow cytometry plots are shown (Lin^{-} cells in panel D). (F-H,K) The livers collected 35 days after transplantation were subjected to H&E staining (F), immunohistochemistry for Ter119 (G), and Berlin blue staining (K). The peripheral blood collected 22 days after transplantation was subjected to May-Grunwald-Giemsa staining (H). Representative pictures are shown. The areas enclosed in the black squares were enlarged (F,K). Arrows indicate stomatocytes (H). (I) A representative picture of the spleens collected 35 days after transplantation is shown. (J) The bilirubin concentration in the serum at indicated days after transplantation was determined by using the UnaG protein (control: n = 4

Stomatocytes are observed in several types of inherited and acquired hemolytic anemia.[34] We found that the serum from *Ehbp1l1*$^{-/-}$ mice exhibited a strong yellow color compared with those from control mice (Figure 5B). We assumed that this was because of an increase in indirect bilirubin caused by aberrant hemolysis. To examine this possibility, we took advantage of UnaG, which is a fluorescent protein that specifically binds to indirect bilirubin,[35,36] and found that serum indirect bilirubin was significantly increased in *Ehbp1l1*$^{-/-}$ mice (Figure 5C). In addition, iron deposition, which is one of the hallmarks of hemolytic anemia, was substantially increased in the livers of *Ehbp1l1*$^{-/-}$ mice compared with control mice (Figure 5D). These results indicate that EHBP1L1 plays an important role in not only regulating erythroblast enucleation but also maintaining the morphology and stability of erythrocytes.

EHBP1L1 in hematopoietic cells is critical for erythropoiesis

To further prove the role of EHBP1L1 in erythroblast enucleation and in maintaining the morphology and stability of erythrocytes, we transplanted either control or *Ehbp1l1*$^{-/-}$ fetal liver cells (FLCs) into irradiated wild-type mice. The blood cell number in *Ehbp1l1*$^{-/-}$ FLC-transplanted mice started to decrease 12 days after transplantation (Figure 6A). In addition, nucleated erythrocytes started to appear in the peripheral blood of *Ehbp1l1*$^{-/-}$ FLC-transplanted mice 22 days after transplantation (Figure 6B-C). As the percentage of nucleated erythrocytes in the peripheral blood of these mice was much lower than that in *Ehbp1l1*$^{-/-}$ mice (Figure 2B-C), we examined the erythroid cell population in the bone marrow. We found that enucleation was significantly impaired in *Ehbp1l1*$^{-/-}$ FLC-transplanted mice (Figure 6D-E; supplemental Figure 7A). Moreover, a large number of nucleated Ter119^{+} cells were accumulated in the livers of *Ehbp1l1*$^{-/-}$ FLC-transplanted mice (Figure 6F-G). This may be because of the disposal of abnormal erythrocytes and iron recycling.[37] Furthermore, we found that many enucleated erythrocytes in *Ehbp1l1*$^{-/-}$ FLC-transplanted mice exhibited stomatocytic morphology (Figure 6H). *Ehbp1l1*$^{-/-}$ FLC-transplanted mice exhibited the following hallmarks of hemolytic anemia: splenomegaly, high serum bilirubin levels, and substantial iron deposition in the liver (Figure 6I-K). Disorganization of splenic architecture with an increased number of erythroid cells was observed in *Ehbp1l1*$^{-/-}$ FLC-transplanted mice, suggesting extramedullary hematopoiesis in response to anemia (supplemental Figure 7B-C). Taken together, EHBP1L1 in hematopoietic cells plays a crucial role in erythroblast enucleation and in maintaining the morphology and stability of erythrocytes.

EHBP1L1 is involved in nuclear positioning in skeletal muscle cells

Centronuclear myopathy is a congenital neuromuscular disorder characterized by severe muscle weakness and hypotonia associated with centralized nuclei and a central accumulation of mitochondria in myofibers.[38] Two downstream effectors of EHBP1L1, Bin1 and dynamin 2, are the causative genes of this disease.[39,40] Therefore, we examined the nuclear localization in myofibers from *Ehbp1l1*$^{-/-}$ embryos. HE staining of hindlimb muscles revealed that the number of skeletal muscle cells with centralized nuclei was significantly increased in *Ehbp1l1*$^{-/-}$ mice (Figure 7A). In contrast, no apparent histological defects, including mislocalization of the nucleus in the small intestine, brain, and retina, were observed in *Ehbp1l1*$^{-/-}$ mice (supplemental Figure 8A-C). In addition, immunofluorescence analysis using an antibody against COX4, a mitochondrial marker, showed a central accumulation of mitochondria in *Ehbp1l1*$^{-/-}$ skeletal muscle cells (Figure 7B). Mitochondrial localization in enucleating erythroblasts was unaffected by the absence of EHBP1L1 (supplemental Figure 8D).[41] These results indicate that EHBP1L1 plays an important role in organelle positioning in a tissue- or cell-type–specific manner.

Discussion

Erythropoiesis is a complex, multistep process that involves the differentiation of erythroid progenitors into mature erythrocytes. This process is tightly regulated by several regulators, such as cytokines and transcription factors. Defects in each of these regulators impair erythropoiesis at various stages of differentiation. Here, we found that the loss of EHBP1L1 caused a defect in erythroblast enucleation because of impaired nuclear polarization, whereas it did not affect the early stages of erythropoiesis. In addition, enucleated erythrocytes in *Ehbp1l1*$^{-/-}$ mice exhibited stomatocytic morphology and were prone to hemolysis. Thus, EHBP1L1 is a novel regulator of the late stages of erythropoiesis (Figure 7C).

GATA1 and KLF1 are the master transcription factors that regulate erythroid differentiation.[42] Genome-wide transcriptome analyses have shown that the expression of EHBP1L1 is reduced in *Klf1*$^{-/-}$ fetal livers[43,44] and increased by the inducible expression of GATA1 in *Gata1*$^{-/-}$ erythroid cells.[45] Furthermore, chromatin immunoprecipitation followed by massively parallel sequencing (chromatin immunoprecipitation-seq) for KLF1 and GATA1 showed that these transcription factors bind to the region near the transcription start site of the *Ehbp1l1* gene in erythroid cells.[45-47] These results suggest that the expression of EHBP1L1 in erythroid cells is directly regulated by these transcription factors. Our results showed that the expression of EHBP1L1 in erythroid cells gradually increased during erythropoiesis. Because KLF1 and GATA1 are expressed and function in erythroid cells throughout erythropoiesis, other layers of regulation probably contribute to the gradual increase in EHBP1L1 expression.

Erythroblast enucleation is a complex sequential process in which the nucleus becomes condensed and polarized to 1 side of orthochromatic erythroblasts and is finally extruded. In enucleating erythroblasts, multiple vesicles are observed in the cytosol, some of which accumulate in the region near the extruding nucleus.[15,16] In addition, treatment with various inhibitors of membrane trafficking and downregulation of clathrin-mediated endocytosis substantially reduce the efficiency of enucleation.[16,17] These observations suggest that the provision of membranes to the cleavage site facilitates nuclear extrusion, which occurs after nuclear polarization. However, we found that the loss of EHBP1L1 impaired nuclear

Figure 6 (continued) and *Ehbp1l1*$^{-/-}$: n = 4). Scale bars: 200 and 50 μm in enlarged pictures for panels F,K, 10 μm for panels G-H, 1 cm for panel I. The data are presented as means ± SEMs for panels A,C,E,J. $^{**}P < .01$, $^{***}P < .001$, $^{****}P < .0001$ (2-way ANOVA in panels A,C,J; unpaired *t* test with Welch's correction in panel E).

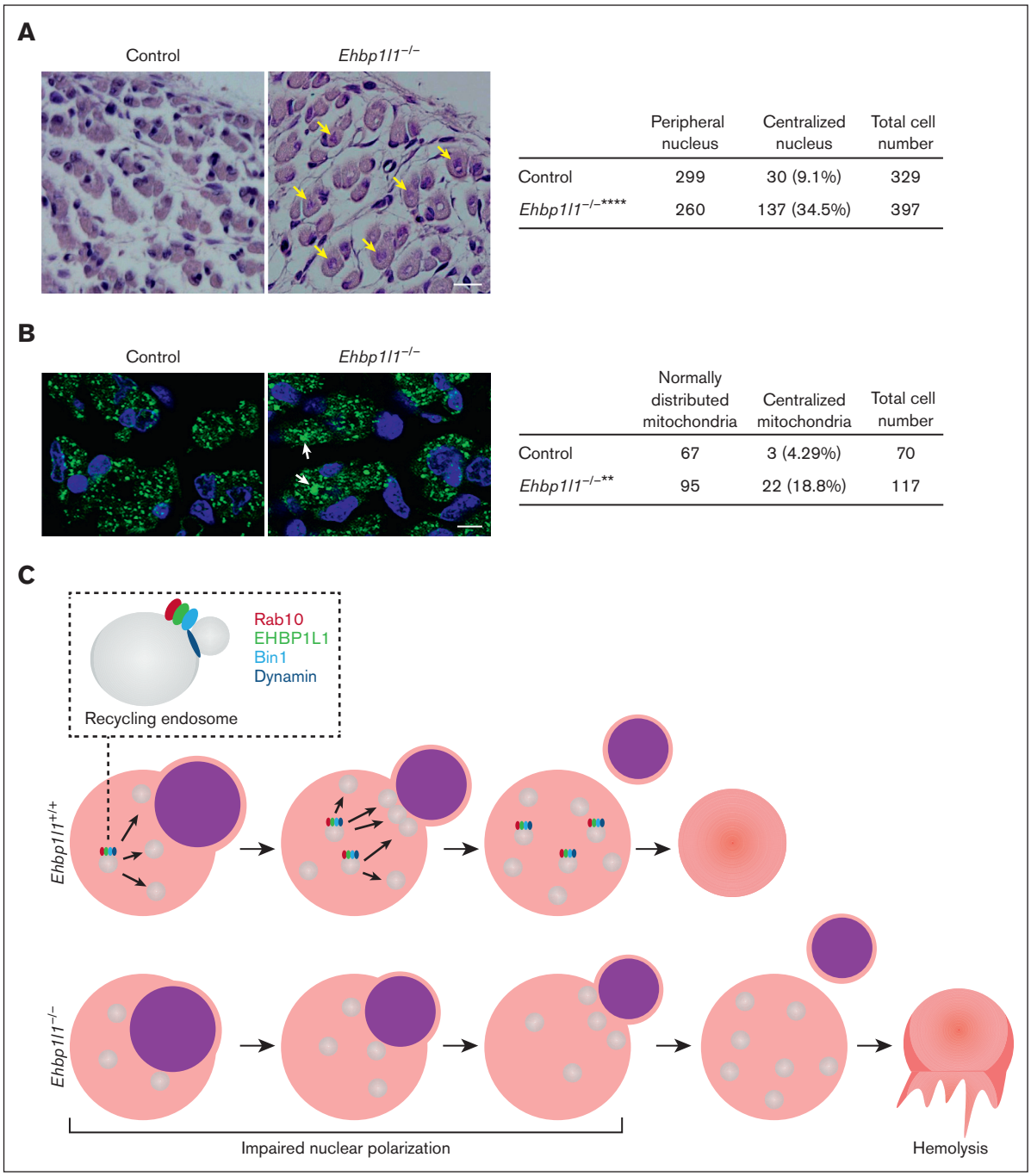

	Peripheral nucleus	Centralized nucleus	Total cell number
Control	299	30 (9.1%)	329
Ehbp1l1$^{-/-}$****	260	137 (34.5%)	397

	Normally distributed mitochondria	Centralized mitochondria	Total cell number
Control	67	3 (4.29%)	70
Ehbp1l1$^{-/-}$**	95	22 (18.8%)	117

Figure 7. Loss of EHBP1L1 causes abnormal central positioning of nuclei and mitochondria in skeletal muscle cells. (A-B) Representative images of HE staining (A) and immunofluorescence staining for the mitochondrial marker COXIV (B) in hindlimb muscles from E18.5 embryos are shown. The numbers of skeletal muscle cells with centralized nuclei (yellow arrows in panel A) and centrally accumulated mitochondria (white arrows in panel B) were determined (6 visual fields for each genotype in panel A; 4 visual fields for control mice and 5 visual fields for *Ehbp1l1*$^{-/-}$ mice in panel B). Bars: 20 μm for panel A and 10 μm for panel B. $^{**}P < .01$, $^{****}P < .0001$ (Fisher exact test). (C) A schematic diagram illustrating the function of EHBP1L1 in terminal erythropoiesis is shown.

polarization, indicating that membrane trafficking plays an important role in not only nuclear extrusion but also nuclear polarization. The surface area of the plasma membrane needs to be increased during nuclear polarization, which is likely supported by membrane trafficking. The fact that nuclear polarization followed by enucleation was not fully blocked by the null mutation of *Ehbp1l1* suggests that these events can proceed in an EHBP1L1-independent manner, although inefficiently. Elucidation of the membrane trafficking machinery during nuclear polarization will facilitate our understanding of erythroblast enucleation.

We found that knockdown of Rab10 and Bin1 suppressed erythroblast enucleation. Treatment with dynamin inhibitors also blocked erythroblast enucleation, as reported in a previous study.[16] Our previous studies showed the critical role of the Rab8-EHBP1L1-Bin1-dynamin axis in epithelial apical transport.[20] In addition, EHBP1L1 directly interacts with Rab10.[27,28] Therefore, EHBP1L1 likely coordinates with Rab10, Bin1, and dynamin to facilitate enucleation. Constitutive deletion of Rab10 or dynamin 2, which is a member of the dynamin family expressed in erythroblasts, results in early embryonic lethality before the initiation of definitive erythropoiesis.[48,49] Similar to *Ehbp1l1*$^{-/-}$ mice, *Bin1*$^{-/-}$ mice died within 24 hours of birth.[50] Although *Bin1*$^{-/-}$ mice were shown to develop ventricular cardiomyopathy, erythroblast enucleation has not been examined in these mice. Therefore, the generation of mice with erythroid-specific knockout of Rab10 and dynamin 2 and a detailed analysis of erythroblast enucleation in these mice will further elucidate the role of the Rab10-EHBP1L1-Bin1-dynamin 2 axis in erythropoiesis.

We found that enucleated erythrocytes in *Ehbp1l1*$^{-/-}$ mice exhibited stomatocytic morphology and were prone to hemolysis. Stomatocytosis is a hemolytic disorder characterized by abnormal ion permeability and cellular hydration.[51] Mutations in various plasma membrane transporters have been identified in patients with this disease. Thus, one can hypothesize that EHBP1L1 regulates the trafficking of these transporters and their regulators to the plasma membrane of erythrocytes. Although Band3 and β1-integrin were properly distributed during enucleation in *Ehbp1l1*$^{-/-}$ erythroblasts, the segregation of other proteins between reticulocytes and pyrenocytes may be disturbed by the loss of EHBP1L1. In addition, as EHBP1L1 is the most highly expressed in reticulocytes among erythroid cells, it might contribute to the final maturation process, including membrane remodeling in reticulocytes. Further studies on these possibilities are warranted.

Bin1 and dynamin 2 are causative genes of centronuclear myopathy, a disorder characterized by the mislocalization of nuclei and mitochondria to the center of myofibers.[39,40] We found similar mislocalization of nuclei and mitochondria in EHBP1L1-deficient myofibers, suggesting that EHBP1L1 is a potential causative gene for this disease. Although genetic mutations in *EHBP1L1* have not been identified in human patients with anemia or centronuclear myopathy, a recent molecular autopsy study in the context of premature death identified an *EHBP1L1* mutation in 2 families with nonimmune fetal hydrops, resulting in recurrent miscarriage.[52] Hydrops fetalis is a serious fetal condition characterized by the abnormal accumulation of fluid in multiple compartments of the fetal body.[53] Disorders of normal erythrocyte production are one of the common etiologies of nonimmune fetal hydrops. Therefore, the *EHBP1L1* mutation might cause lethal hemolytic anemia, leading to fetal loss in patients with this condition. Very recent studies have identified an *EHBP1L1* mutation in a pedigree of dogs that exhibited anemia and myopathy.[54,55] Furthermore, loss-of-function mutations in genes involved in membrane trafficking, such as *SEC23B* and *VPS4A*, have been identified in patients with congenital dyserythropoietic anemia.[56-58] Although the functional interactions between EHBPL1 and these proteins remain unknown, these cases highlight the importance of the membrane trafficking machinery in erythropoiesis. Understanding the mechanism underlying EHBP1L1-mediated establishment and maintenance of permanent and transient cell polarity in various cell types will provide insights into the pathogenesis of diseases associated with cell polarity.

Acknowledgments

The authors thank Yuichiro Hara (Tokyo Metropolitan Institute of Medical Science) for assistance with the analysis of the public chromatin immunoprecipitation sequencing data, Kyowa Hakko Kirin for kindly providing erythropoietin, and Institute of Experimental Animal Sciences (Graduate School of Medicine, Osaka University) for assistance with animal experiments.

This study was supported by the Japan Society for the Promotion of Science KAKENHI grants 17H06422, 19K22514, and 21H02658 (A.H.), grants from SENSHIN Medical Research Foundation (K.M. and S.K.), and JST SPRING (JPMJSP2138 [J.W.]).

Authorship

Contribution: A.H. conceived of the project; J.W., K.M., T.A., and S.K. designed and performed experiments; R.N. and N.H. assisted in performing the transplantation experiment; M.T. performed the histological analysis; M.K. assisted in maintaining mice; J.W., K.M., T.A., R.N., S.K., T.S., S.-i.Y., M.K., T.N., N.H., E.M., and A.H. analyzed the data; J.W. and K.M. drafted the manuscript; K.M. and A.H. edited the manuscript; and K.M. and A.H. supervised the study.

Conflict-of-interest disclosure: The authors declare no competing financial interests.

ORCID profiles: J.W., 0000-0001-6378-2431; K.M., 0000-0002-8724-4715; R.N., 0000-0002-7891-4879; S.K., 0000-0002-1123-1205; S.-i.Y., 0000-0003-3632-0674; M.K., 0000-0001-7222-7456; E.M., 0000-0002-9430-2362.

Correspondence: Kenta Moriwaki, Department of Biochemistry, Toho University School of Medicine, 5-21-16, Omorinishi, Otaku, Tokyo 143-8540, Japan; email: kenta.moriwaki@med.toho-u.ac.jp; and Akihiro Harada, Department of Cell Biology, Graduate School of Medicine, Osaka University, 2-2, Yamadaoka, Suita 565-0871, Japan; email: aharada@acb.med.osaka-u.ac.jp.

References

1. Campanale JP, Sun TY, Montell DJ. Development and dynamics of cell polarity at a glance. *J Cell Sci*. 2017;130(7):1201-1207.
2. Wodarz A, Nathke I. Cell polarity in development and cancer. *Nat Cell Biol*. 2007;9(9):1016-1024.
3. Gundersen GG, Worman HJ. Nuclear positioning. *Cell*. 2013;152(6):1376-1389.
4. Dzierzak E, Philipsen S. Erythropoiesis: development and differentiation. *Cold Spring Harb Perspect Med*. 2013;3(4):a011601.

5. Menon V, Ghaffari S. Erythroid enucleation: a gateway into a "bloody" world. *Exp Hematol*. 2021;95:13-22.
6. Ji P, Yeh V, Ramirez T, Murata-Hori M, Lodish HF. Histone deacetylase 2 is required for chromatin condensation and subsequent enucleation of cultured mouse fetal erythroblasts. *Haematologica*. 2010;95(12):2013-2021.
7. Wang Y, Li W, Schulz VP, et al. Impairment of human terminal erythroid differentiation by histone deacetylase 5 deficiency. *Blood*. 2021;138(17):1615-1627.
8. Ji P, Jayapal SR, Lodish HF. Enucleation of cultured mouse fetal erythroblasts requires Rac GTPases and mDia2. *Nat Cell Biol*. 2008;10(3):314-321.
9. Konstantinidis DG, Pushkaran S, Johnson JF, et al. Signaling and cytoskeletal requirements in erythroblast enucleation. *Blood*. 2012;119(25):6118-6127.
10. Ubukawa K, Guo YM, Takahashi M, et al. Enucleation of human erythroblasts involves non-muscle myosin IIB. *Blood*. 2012;119(4):1036-1044.
11. Kobayashi I, Ubukawa K, Sugawara K, et al. Erythroblast enucleation is a dynein-dependent process. *Exp Hematol*. 2016;44(4):247-256.e12.
12. Nowak RB, Papoin J, Gokhin DS, et al. Tropomodulin 1 controls erythroblast enucleation via regulation of F-actin in the enucleosome. *Blood*. 2017;130(9):1144-1155.
13. Ubukawa K, Goto T, Asanuma K, et al. Cdc42 regulates cell polarization and contractile actomyosin rings during terminal differentiation of human erythroblasts. *Sci Rep*. 2020;10(1):11806.
14. Wang J, Ramirez T, Ji P, Jayapal SR, Lodish HF, Murata-Hori M. Mammalian erythroblast enucleation requires PI3K-dependent cell polarization. *J Cell Sci*. 2012;125(pt 2):340-349.
15. Iacopetta BJ, Morgan EH, Yeoh GC. Receptor-mediated endocytosis of transferrin by developing erythroid cells from the fetal rat liver. *J Histochem Cytochem*. 1983;31(2):336-344.
16. Keerthivasan G, Small S, Liu H, Wickrema A, Crispino JD. Vesicle trafficking plays a novel role in erythroblast enucleation. *Blood*. 2010;116(17):3331-3340.
17. Keerthivasan G, Liu H, Gump JM, Dowdy SF, Wickrema A, Crispino JD. A novel role for survivin in erythroblast enucleation. *Haematologica*. 2012;97(10):1471-1479.
18. Sato T, Iwano T, Kunii M, et al. Rab8a and Rab8b are essential for several apical transport pathways but insufficient for ciliogenesis. *J Cell Sci*. 2014;127(pt 2):422-431.
19. Sato T, Mushiake S, Kato Y, et al. The Rab8 GTPase regulates apical protein localization in intestinal cells. *Nature*. 2007;448(7151):366-369.
20. Nakajo A, Yoshimura SI, Togawa H, et al. EHBP1L1 coordinates Rab8 and Bin1 to regulate apical-directed transport in polarized epithelial cells. *J Cell Biol*. 2016;212(3):297-306.
21. Hiroyama T, Miharada K, Sudo K, Danjo I, Aoki N, Nakamura Y. Establishment of mouse embryonic stem cell-derived erythroid progenitor cell lines able to produce functional red blood cells. *PLoS One*. 2008;3(2):e1544.
22. Sankaran VG, Xu J, Orkin SH. Advances in the understanding of haemoglobin switching. *Br J Haematol*. 2010;149(2):181-194.
23. Liu J, Zhang J, Ginzburg Y, et al. Quantitative analysis of murine terminal erythroid differentiation in vivo: novel method to study normal and disordered erythropoiesis. *Blood*. 2013;121(8):e43-e49.
24. Chen K, Liu J, Heck S, Chasis JA, An X, Mohandas N. Resolving the distinct stages in erythroid differentiation based on dynamic changes in membrane protein expression during erythropoiesis. *Proc Natl Acad Sci U S A*. 2009;106(41):17413-17418.
25. Yoshida H, Kawane K, Koike M, Mori Y, Uchiyama Y, Nagata S. Phosphatidylserine-dependent engulfment by macrophages of nuclei from erythroid precursor cells. *Nature*. 2005;437(7059):754-758.
26. Koury ST, Koury MJ, Bondurant MC. Cytoskeletal distribution and function during the maturation and enucleation of mammalian erythroblasts. *J Cell Biol*. 1989;109(6 pt 1):3005-3013.
27. Rai A, Oprisko A, Campos J, et al. bMERB domains are bivalent Rab8 family effectors evolved by gene duplication. *Elife*. 2016;5:e18675.
28. Liu Z, Xu E, Zhao HT, Cole T, West AB. LRRK2 and Rab10 coordinate macropinocytosis to mediate immunological responses in phagocytes. *EMBO J*. 2020;39(20):e104862.
29. An X, Schulz VP, Li J, et al. Global transcriptome analyses of human and murine terminal erythroid differentiation. *Blood*. 2014;123(22):3466-3477.
30. Paralkar VR, Mishra T, Luan J, et al. Lineage and species-specific long noncoding RNAs during erythro-megakaryocytic development. *Blood*. 2014;123(12):1927-1937.
31. Gautier EF, Ducamp S, Leduc M, et al. Comprehensive proteomic analysis of human erythropoiesis. *Cell Rep*. 2016;16(5):1470-1484.
32. Park RJ, Shen H, Liu L, Liu X, Ferguson SM, De Camilli P. Dynamin triple knockout cells reveal off target effects of commonly used dynamin inhibitors. *J Cell Sci*. 2013;126(pt 22):5305-5312.
33. McCluskey A, Daniel JA, Hadzic G, et al. Building a better dynasore: the dyngo compounds potently inhibit dynamin and endocytosis. *Traffic*. 2013;14(12):1272-1289.
34. Gallagher PG. Disorders of erythrocyte hydration. *Blood*. 2017;130(25):2699-2708.
35. Kumagai A, Ando R, Miyatake H, et al. A bilirubin-inducible fluorescent protein from eel muscle. *Cell*. 2013;153(7):1602-1611.
36. Iwatani S, Nakamura H, Kurokawa D, et al. Fluorescent protein-based detection of unconjugated bilirubin in newborn serum. *Sci Rep*. 2016;6:28489.

37. Theurl I, Hilgendorf I, Nairz M, et al. On-demand erythrocyte disposal and iron recycling requires transient macrophages in the liver. *Nat Med*. 2016;22(8):945-951.

38. Jungbluth H, Gautel M. Pathogenic mechanisms in centronuclear myopathies. *Front Aging Neurosci*. 2014;6:339.

39. Bitoun M, Maugenre S, Jeannet PY, et al. Mutations in dynamin 2 cause dominant centronuclear myopathy. *Nat Genet*. 2005;37(11):1207-1209.

40. Nicot AS, Toussaint A, Tosch V, et al. Mutations in amphiphysin 2 (BIN1) disrupt interaction with dynamin 2 and cause autosomal recessive centronuclear myopathy. *Nat Genet*. 2007;39(9):1134-1139.

41. Liang R, Menon V, Qiu J, et al. Mitochondrial localization and moderated activity are key to murine erythroid enucleation. *Blood Adv*. 2021;5(10):2490-2504.

42. Barbarani G, Fugazza C, Strouboulis J, Ronchi AE. The pleiotropic effects of GATA1 and KLF1 in physiological erythropoiesis and in dyserythropoietic disorders. *Front Physiol*. 2019;10:91.

43. Tallack MR, Magor GW, Dartigues B, et al. Novel roles for KLF1 in erythropoiesis revealed by mRNA-seq. *Genome Res*. 2012;22(12):2385-2398.

44. Hung CH, Lee TL, Huang AY, et al. A positive regulatory feedback loop between EKLF/KLF1 and TAL1/SCL sustaining the erythropoiesis. *Int J Mol Sci*. 2021;22(15):8024.

45. Cheng Y, Wu W, Kumar SA, et al. Erythroid GATA1 function revealed by genome-wide analysis of transcription factor occupancy, histone modifications, and mRNA expression. *Genome Res*. 2009;19(12):2172-2184.

46. Tallack MR, Whitington T, Yuen WS, et al. A global role for KLF1 in erythropoiesis revealed by ChIP-seq in primary erythroid cells. *Genome Res*. 2010;20(8):1052-1063.

47. Pilon AM, Ajay SS, Kumar SA, et al. Genome-wide ChIP-seq reveals a dramatic shift in the binding of the transcription factor erythroid Kruppel-like factor during erythrocyte differentiation. *Blood*. 2011;118(17):e139-148.

48. Lv P, Sheng Y, Zhao Z, et al. Targeted disruption of Rab10 causes early embryonic lethality. *Protein Cell*. 2015;6(6):463-467.

49. Ferguson SM, Raimondi A, Paradise S, et al. Coordinated actions of actin and BAR proteins upstream of dynamin at endocytic clathrin-coated pits. *Dev Cell*. 2009;17(6):811-822.

50. Muller AJ, Baker JF, DuHadaway JB, et al. Targeted disruption of the murine Bin1/Amphiphysin II gene does not disable endocytosis but results in embryonic cardiomyopathy with aberrant myofibril formation. *Mol Cell Biol*. 2003;23(12):4295-4306.

51. Andolfo I, Russo R, Gambale A, Iolascon A. Hereditary stomatocytosis: an underdiagnosed condition. *Am J Hematol*. 2018;93(1):107-121.

52. Shamseldin HE, AlAbdi L, Maddirevula S, et al. Lethal variants in humans: lessons learned from a large molecular autopsy cohort. *Genome Med*. 2021;13(1):161.

53. Swearingen C, Colvin ZA, Leuthner SR. Nonimmune hydrops fetalis. *Clin Perinatol*. 2020;47(1):105-121.

54. Thomas-Hollands A, Shelton GD, Guo LT, et al. Congenital dyserythropoiesis and polymyopathy without cardiac disease in male Labrador retriever littermates. *J Vet Intern Med*. 2021;35(5):2409-2414.

55. Shelton GD, Minor KM, Guo LT, et al. An EHPB1L1 nonsense mutation associated with congenital dyserythropoietic anemia and polymyopathy in Labrador retriever littermates. *Genes*. 2022;13(8):1427.

56. King R, Gallagher PJ, Khoriaty R. The congenital dyserythropoieitic anemias: genetics and pathophysiology. *Curr Opin Hematol*. 2022;29(3):126-136.

57. Schwarz K, Iolascon A, Verissimo F, et al. Mutations affecting the secretory COPII coat component SEC23B cause congenital dyserythropoietic anemia type II. *Nat Genet*. 2009;41(8):936-940.

58. Seu KG, Trump LR, Emberesh S, et al. VPS4A mutations in humans cause syndromic congenital dyserythropoietic anemia due to cytokinesis and trafficking defects. *Am J Hum Genet*. 2020;107(6):1149-1156.